ISSN (Print): 0974-6846
Indian Journal of Science and Technology, *Vol 11(37), DOI: 10.17485/ijst/2018/v11i37/130226, October 2018* ISSN (Online): 0974-5645

Determination of the Degree of Saturation and Chloride Penetration in Cracked Hydraulic Concrete Structures: Using Developed Electrical Conductivity Technique

Thair Jabar Mizhir Alfatlawi and Riyadh Abdulabbas Ali Alsultani*

Faculty of Civil Engineering, University of Babylon, Babil - 51001, Iraq;
stud.reyadabedalabasali93@uobabylon.edu.iq, eng.thair.jabbber@uobabylon.edu.iq

Abstract

Objectives: Determination of the degree of saturation and chloride penetration in cracked hydraulic concrete structures. **Methods**: Depending on Electrical Conductivity (EC) principle, developed method called Electrical Conductivity Technique (ECT), was submitted for purposes of evaluating and calculating the accurate degree of saturation and amount of chloride penetration in mentioned structures. Many experimental specimens were used for test this method and compered with numerical result. **Findings:** The experimental results were obtained by using this new test, agreed fairly with results which obtained from numerical solutions. So the developed ECT is the more suitable method for determining the degree of saturation and penetration of chloride ions in the laboratory. **Application/Improvement:** This research ensures a novel application for the use of the electrical conductivity principles to find the chloride concentrations in the concrete model with a very precise manner, which contributes to better understanding of the penetration processes in terms of salts or saturation within the concrete structures.

Keywords: Artificial Crack, Chloride Penetration, Marine Environment, Developed Electrical Conductivity Technique (ECT), Hydraulic Concrete Structures (HCS)

1. Introduction

Concrete is one of the most widely material that used in hydraulic structures for the purpose of controlling the water resources. With properly design and produce, it is an extremely durable material with a service life up to 100 years. However, under certain environmental conditions the service life of reinforced concrete structures is more limited[1, 2]. Seawater represents one of the most severe natural environments in the world that contains some aggressive agents that are very harmful to concrete materials. For different reasons, concrete structures are frequently cracked, the presence of cracks in those structures play an important catalyzer role of diminution of service life of steel bars and producing loss of structural strength, stability and durability[3].

Electromagnetic techniques are sensitive to these aggressive agents and can be used to assess concrete durability in terms of the degree of saturation and presence of chloride ions into concrete body. One of the most popular techniques is the Electrical Conductivity (EC) of test specimens. There are many test procedures have been developed to determine the EC of the concrete specimens. They are reviewed in various publications such as[4-6]. Two-plate configurations are often used in the laboratory where specimens are of uniform geometry[7-9], whereas four-point surface techniques such as the Wenner technique[10] are popular for in situ applications[11-15].

All these methods give an indication of concrete's resistance to the chloride ion penetration. However, the information provide by these tests are limited and also they can't determine the exact distribution of the chloride

*Author for correspondence

penetration because it works on external inspection of the concrete. The problem is particularly most common for calculating the accurate depth of the chloride distribution into concrete structures. So this study aims to develop a method to locate the chloride ions penetration experimentally and compared these results with numerically results.

The laboratory experimental aims to study the influence of cracks on the chloride penetration of concrete specimens with (250 × 250 × 250) mm dimensions and with artificial crack. The specimens were pre-cracked, using a shim copper plate to create cracks in the Middle dimension of specimens, with a dimensions (1 and 2) mm as crack widths and (6 and 10) cm as crack depth. Therefore, the chloride distribution profile was monitored by using a developed ECT at 0 hour and after 312 hours (13 days) of exposure to 2 m as water head coupled with 3.5% NaCl to simulate the typical marine environment of seawater[16].

Numerical results were obtained using a developed two dimensional model with finite element analysis (Comsol Multiphysics Software), by simulating chloride penetration depth in cracked concrete considering the real microstructure including cement paste, voids and aggregates.

Comparisons between the results on chloride penetration concluded that the numerical ones obtained, using the mass diffusion and convection modulus with Darcy's law, conformable with the experimental ones which analyzed as 2D-colour images with Matlab Software.

2. Experimental Program

2.1 Chloride Ion Transport

Chloride transport in concrete is a complex process, involving mechanisms such as diffusion, convection, capillary suction or by any combination of these, flow with flowing water, accompanied by physical and chemical binding[17].

The governing mechanisms of transport in Hydraulic Concrete Structures depend on the exposure conditions and transport mechanisms embodiment in water-retaining structures because of a water pressure which applied, by water head, on apparent face of it structures. Since this study studies the ingress of chloride ions in submerged cracked concrete structures, so that the most important and often governing transport processes, in these fully or semi-fully water saturated structures, are convection and diffusion[18].

Under saturated conditions, as submerged members of concrete structures which are exposed to a marine environment, water flow is driven by a pressure gradient according to Darcy's law. Darcy's Law can also be expressed in terms of pressure head with the relation of pressure p to the total hydraulic head H or the pressure head H_p:

$$H = H_p + D \quad (1)$$

Where: H: hydrostatic head, H_p: pressure head and D: elevation head.

2.2 Concrete Composition

Based on the standard specifications and conforming to ASTM C595, most of the concrete structures exposed to the marine environment must be used blended cement, low water/binder ratio, upper than 5% of silica fume and high value of compressive strength, as an appropriate concrete mixture[19-21], so that depending on the recommended raw materials characterization and concrete mixture features, the concrete mixture utilized in all experimental specimens are report in Table 1:
The concrete samples were cast as:

- Four cracked cubic specimens (250 × 250 × 250) mm.
- Eight cubic samples (75 × 75 × 50) mm, for calibration of the EC.

All these samples were done with a same mixture and as reported in Table 1. After 24 hours of covered samples with polyethylene sheets to prevent moisture loss from

Table 1. Mixing proportion of concrete materials and concrete properties (adopted from[22])

Cement (kg/m^3)	450
Silica fume (kg/m^3)	32
Fine aggregate (kg/m^3)	1232
Coarse aggregate (kg/m^3)	410
Water (kg/m^3)	169
Super plasticizer (kg/m^3)	7
Water/binder ratio (%)	35
Slump (cm)	10–12
28-day compressive strength (MPa)	50

the concrete, then they were named and submerged in a filled water basin in the curing room with a temperature 23 ± 2C° and RH > 90% for 28 days.

2.3 Probe Preparation

2.3.1 Probes type

A smoothly surface brass probes, to ensure close touch between the probes and concrete specimens[7, 23-24], were used and developed to find the least disturbance of chloride penetration in the concrete specimens. According to simplest EC waves of the two-probe configuration as shown in Figure 1, so 12 × 13 probes, grid map covered an area of 525 cm^2 around the crack, were inserted and selected as data points to acquire the best resolution of the chloride penetration in concrete specimens.

2.3.2 Probes length, diameter and spacing

In the current study, a 255 mm probe length was selected as short enough lengths to fit on most concrete specimens are shown in Figure 2. The probe was carefully chosen with diameter d = 2.5 mm, spacing D = 20 mm to satisfy the mapping of the probes matrix within the cubic concrete specimens.

2.3.3 Probes installation

In order to gain the exact profile of chloride location, the probes were embedded from the side surface of the specimens; therefore a timber probe holder was intended to keep the probes parallel to each other and vertical to the surface of concrete specimen (Figure 3a and b). The edges of those holes were made with chamfers which enabled the probes to effortlessly go through.

2.4 Creation of Cracks

Concrete specimens were cast with two levels of crack depth and width. Cracks were created by molding concrete with a thin copper plate (shims) installed at the center of the mold. Before casting the concrete mixture, shims, with a (250 × 60 and 250 × 100) mm cross section and thicknesses of 1 mm and 2 mm, were linked to the side surface of the mold, as presented in Figure (4a), in order to make the cracks. Through 24 hours curing the plate was dragged out totally.

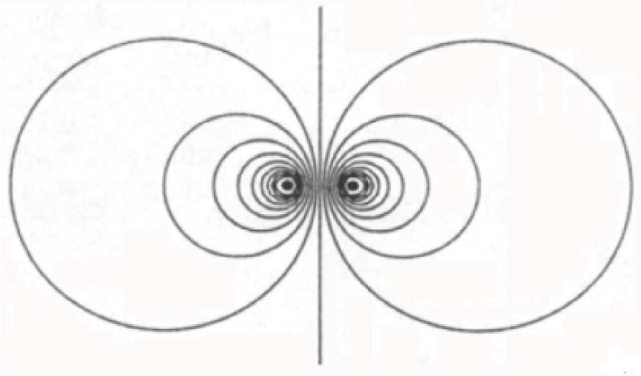

Figure 1. Electrical field lines generated by probe configuration.

Figure 2. Rod probes.

2.5 Coating and Finishing

Following 28 days of putting in the curing basin, the specimens were painted with epoxy, except the finish surface (crack side), which permitted one dimensional transport of chloride solute inherent concrete specimen and was more illustrative of numerous field hydraulic structures.

Before application, all specimens were cleaned by an air compressor blower to remove any dust or debris. Three layers of painting were applied to the specimens to ensure the fill of all open pores in the concrete surfaces (Figure 4b and c). Care was taken to keep the epoxy from filling the cracks.

2.6 Environmental Treatment

Water pressure are applied with head of 2 meter and coupled with 3.5% chloride-sodium, to find the chloride

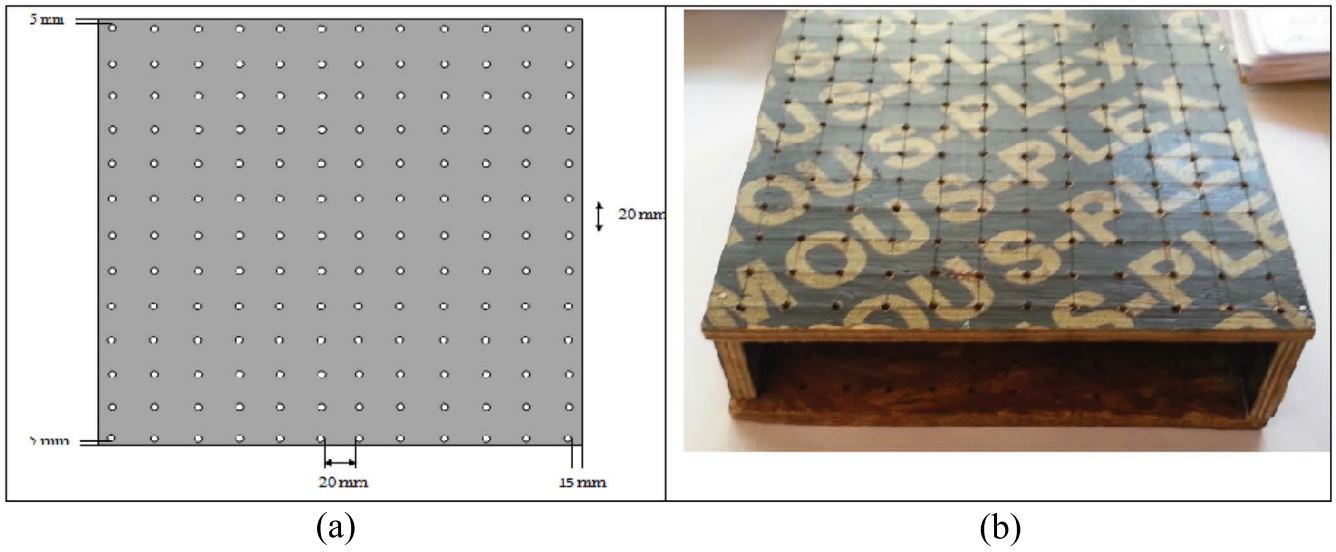

Figure 3. Double-layered probe holder, **(a)** Schematic representation with dimensions. **(b)** Picture of an actual holder.

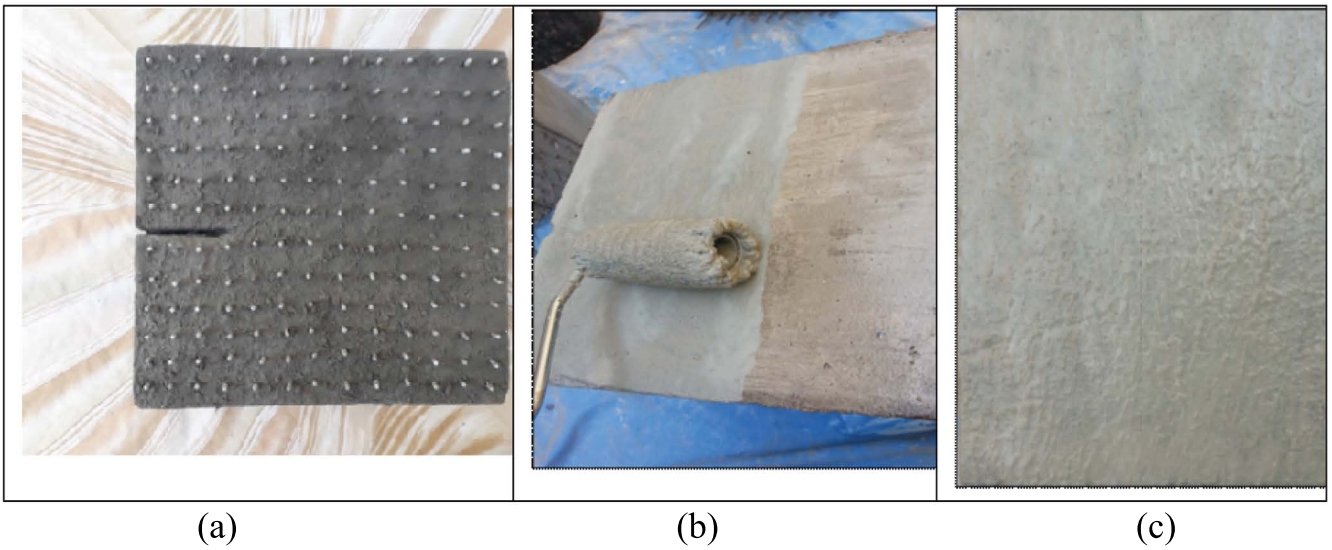

Figure 4. Preparation of specimens **(a)** Creation of crack **(b)** Coating with epoxy **(c)** Final-finished of specimens.

penetration depth into the concrete specimens through uncoated faces over time (312 hrs).

2.7 Electrical Conductivity Test (ECT)

2.7.1 General

The EC of concrete has been the focal point of numerous studies on the past 60 years[7, 11, 23, 25, 26]. They presented that the conductivity of any material is defined as inverted the value of the resistance between the faces corresponding to the cube unit of the material, where their results focused that the EC inherent material properties.

In an attempt to facilitate testing of the chloride penetration in concrete, the ECT was developed by an accurate unique test. The developed ECT was designed, through the implantation of a group of sensitive probes in the concrete specimen and with appropriate dimensions, so that the quantity and location of the chloride penetration into the concrete is found as it actually exists. To eliminate the imbalance in the creation of readings, there are many laws that have been relied upon, of which what is available while others have been developed and adopted in this new sophisticate way.

Ohm's law states that the resistance of any material is defined as:

$$R = V\, I^{-1} \tag{2}$$

Where: R: resistance of material, (ohms); V: applied voltage, (volt) and I: passed current, (amber).
The resistivity of any material is defined as[23]:

$$\rho_{Elec.} = R\, A\, D^{-1} \tag{3}$$

Where: $\rho_{Elec.}$: resistivity of material, (Ω-m); A: cross-sectional area, (m^2) and D: specimen length (distance between two electrodes), (m), so that the resistivity is defined as the resistance of the interior concrete area between each two probes. And as expressed by the new formula:

$$\rho_{Elec.} = R\, A\, D^{-1} = R\left(L * d\right) D^{-1} \tag{4}$$

Where: A: interior concrete cross-sectional area between two probes, (m^2); d diameter of probe, (m); L: length of probe, (m) and D: distance between two probes.

The EC of a porous material is determined as the mutuality of resistivity[27, 28]:

$$\sigma_{Elec.} = \rho_{Elec.}^{-1} \tag{5}$$

Where: $\sigma_{Elec.}$: is the EC of the materials (Siemens/m).

Conductivity being a fundamental property of the material, whereas it is depends upon the shape and size of material.

There are two main types of tests that can be done to determine a concrete resistivity value, involving either a Direct Current (DC) or an Alternating Current (AC)[23, 24]. Direct current resistivity can be measured by applying a voltage between two probes with the concrete sandwiched between them.

The use of a DC voltage results in polarization of the electrolyte and the formation of hydrogen and oxygen gas at the measuring electrodes[23, 24]. This polarization potential opposes the flow and manifests itself in the form of a reduced current for a given applied voltage, V,

$$R = \left(V - V_p\right) I^{-1} \tag{6}$$

Where: V_p: is the polarization potential.

If it is assumed that this polarizing effect is constant at different applied voltages, this effect can be accounted for by taking current measurements at two different applied voltages. The polarization potential is given by equation (7) and as mentioned by[23].

$$V_p = V_1 I_2 - V_2 I_1 \left(I_1 - I_2\right)^{-1} \tag{7}$$

Where: V_1 and V_2 are the two applied voltages, I_1 and I_2 are the corresponding currents.

2.7.2 Test setup

The ECT used direct current-voltage, to characterize the effect of saturation on the chloride penetration, to measure the EC (Equation 5) of the concrete specimens. Conductivity technique consists of a power supply instrument, an electrical multi-meter and tester cables were connected with each other and with stainless probes which embedded in concrete test specimens are shown Figure 5. The EC was measured from the probes grid as each two vertical neighboring probes formed probe pair, which gave 11 × 12 data point.

2.7.3 Electrical conductivity calibration

Eight calibration samples, (75 × 75 × 50) mm, were casted and cured for 28 days. Following that, twelve times of drying were conducted. Each time, the specimens were placed into a 105C° drying oven for 2 hours; the final drying was conducted for 24 hours are shown in Figure 6a. After each drying step, the samples were removed from the oven, wiped, weighted, and then returned to oven drying; finally (after 24 hrs.) the electrical conductivities of all samples were registered. After that, they conditioned in the controlled room and were submerged, wrapped, and sealed in plastic bags, contain a series of NaCl solutions with concentration 0.0%, 0.5%, 1.0%, 1.5%, 2.0%, 2.5%, 3.0% and 3.5% by weight of water is shown in Figure 6b,

Figure 5. Developed ECT instrument.

and kept for three months respectively. The time allowed for the water to equalize conservative; it was decided based on ASTM D2216-10[29] where a much larger cylinder samples were used.

Each sample had a number of distributed probes with L = 55 mm, D = 2.5 mm, d = 20 mm. For each water level, the water contents of the samples were measured by weights and the EC (calibration data) were read at different locations of the samples. However, the developed ECT depending on values data that taken from the calibration samples, geometric constants of the probe configuration used in the ECT test were not taken into account.

3. Experimental Results

3.1 Calibration of Developed ECT

In order to decrease the mistake of EC polarization, two different Voltages (V) were applied to each specimen and the current (I) corresponding to each voltage was measured. The polarization potential was calculated for each set of measurements using equation (7). Once the polarization potential was known, the resistance was obtained using equation (6). The use of higher voltage levels was avoided since the higher voltage produces heat during measurement that could change the saturation of the specimens. It was noticed that the voltage levels (5.0V and 2.5V) were all above the level of polarization potential drop, which is typically ~ 1.8 V.

3.2 Chloride Content and Electrical Conductivity Relation

After the 28 days of the eight samples curing, the electrical conductivities, of each sample, were measured. Water contents (*w)* of samples, according its weight, were recorded during the oven drying steps are shown in Figure 7, and after that the electrical conductivities were measured for all samples. After 90 days of the immersing these samples in the series of chloride solutions and as mentioned earlier. Currents, of the seven steps of EC tests, were made for every 15 days, then collected and converted to electrical conductivities by using equation (5). For each sample, twenty-four readings were made from twenty-four pairs of probes formed by sixteen probes in each sample. Considering the penetration of solutions into the samples during this test, almost two readings near the sample center were not taken into account. For each sample, the results did not show an uneven reading of EC values; therefore, the average value was taken for each sample and test shown in Figure 8.

As seen from the Figure 8, at given water content, samples soaked in fresh water have a lower EC than a sample soaked in salty water. For samples soaked in salt solutions of different concentrations, the σ-*w* curves were drawn together. This fact suggests that the EC results measured by this developed Technique are very sensitive to chloride concentrations in the concrete Medias. From the Ec values of the samples, it can notice the chloride concentration of solution did not fully absorbed in

Figure 6. Calibration of samples **(a)**: Oven drying. **(b):** sealed.

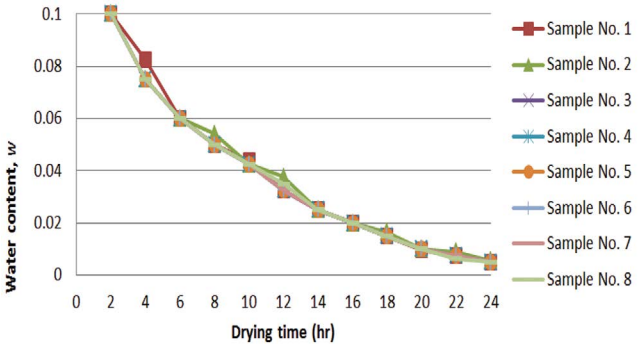

Figure 7. Oven drying and water content change of calibration samples.

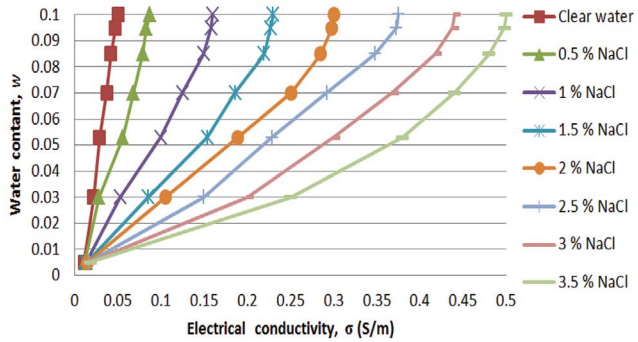

Figure 8. Relationship between chloride contents and electrical conductivities.

samples due to the porous nature of concrete samples. Mathematical analysis of these values was done and the concentrations were converted to corresponding values.

For samples soaked in salt solutions of different concentrations, the σ-*w* curves weave together. This fact suggests that the EC results measured by this developed technique are very sensitive to chloride concentrations in the concrete Medias.

As seen in the same Figure 8, at the end of all tests, there are semi-straight line at the end of each curve, these facts given an indication for the fully saturated samples for every concentration series; therefore these values installed as a true value for each chloride ratio (Table 2).

From the EC values of the samples which presented in the Table 2, we can notice that sample No. 8 who immersed in concentration 3.5% of Nacl solution, has an EC (0.5 S/m) of 2.5% saline solution concentration (0.49 S/m) in addition to the EC of the dried concrete (0.01 S/m), and thus to the rest of the values. This fact attributed to that chloride concentration of solution did not fully absorbe in samples due to the porous nature of concrete samples. Mathematical analysis of these values was done and the concentrations were converted to corresponding values.

For the seven reading data of each sample, a calibration equation was suggested for these results with 0.9963 linear regression value, and as shown Figure 9.

So that the relationship between chloride content (%) and EC (S/m) is can be gotten by the following calibration equation:

$$C_x = 5.3236\,EC - 0.1735 \quad (8)$$

Where: C_x: typical concentration inside specimens.

Therefore, in this project, the EC measurement is a chief used as a supplementary data for the measurement of the chloride contents change inside concrete specimens.

3.3 Change of Chloride Penetration in Specimens

After 28 days of concrete curing, in addition to the 3 hours of coating with epoxy, the concrete specimens can be considered saturated or semi-saturated with water and this is considered as simulation to prototype HCS. The specimens were exposed to 3.5% chloride solution and under

Table 2. Spacemen's details and the electrical conductivity values

NaCl concentration (%)	Av. EC of saline solution (S/m)	Sample's number (No.)	Av. EC of samples (S/m)
0.0 % (tap water)	0.041	1	0.050
0.5 %	0.207	2	0.087
1.0 %	0.278	3	0.160
1.5 %	0.342	4	0.230
2.0 %	0.415	5	0.300
2.5 %	0.490	6	0.375
3.0 %	0.558	7	0.440
3.5 %	0.615	8	0.500

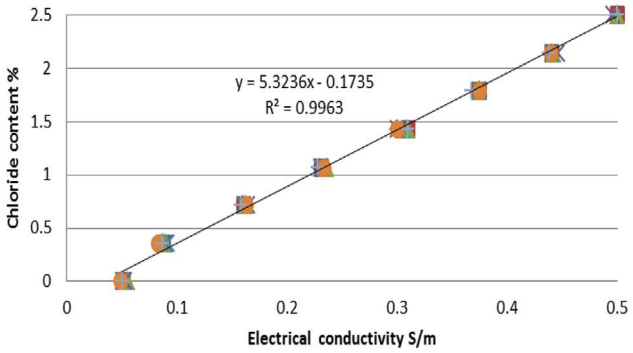

Figure 9. Electrical conductivity verse chloride contents.

required water (solute) head. The chloride content was tested with the developed ECT after coated with epoxy and after 312 hrs. Following the steps described in section 2.7.2. As shown in the Figure 10, the round solid marks indicate the location where probes were inserted. Every two vertical neighboring probes were employed as a two-rod probe pair to send and receive signals by a cable taster connected with conductivity meter. The surrounding lines show the signal distribution and the "x" marks represent the location, for which the chloride content was recorded. It was assumed that the chloride content at locations marked as "x" location was equal to the averaged chloride content for the signal covered area. The matrix of currents data were collected and then converted to EC then to chloride content through the calibration equation 8. The distribution of chloride content in the probed area was presented by color scaled 2D images imported from Matlab software. Among the 282 data points, linear interpolations were employed by Matlab Software to improve the data visualization.

4. Numerical Simulation

The finite element method was used to numerically solve the penetration equation (1). For the numerical simulation, the COMSOL Multiphysics software was used to investigate the chloride penetration in concrete specimens. COMSOL software utilizes Transport of Diluted Species (TDS) to compute the concentration field of convection dilutes solute in a porous material. Numerical solutions of the problem are based on the compressible flow physics solved by Darcy equations for conservation momentum and continuity equation of conservation mass. For a higher coupled flow the non-steady (time-dependent) analyses have been used.

The 2D numerical model was set according to the cracked wall specimens used in the experimental test for purposes of comparison with the model. It consists of specimens with square domain (0.25 m and 0.25 m in width and depth, respectively) representing the concrete wall with a varied crack size at mid of the specimens.

Determining the appropriate grid domain along with a suitable mesh cell size is a critical part of any numerical model simulation. In COMSOL, grid generation is the most user-friendly tools to obtain the accurate solution. If good quality of mesh is generated, one can obtain realistic results from the numerical models. The mesh statistics of all models were meshed into 6776–7226 triangular elements; the number of boundary elements was between 364 and 412.

Figure 11 shows the boundary condition that applied to solve the mathematical equations governs chloride solute penetration into concrete structures. In the model

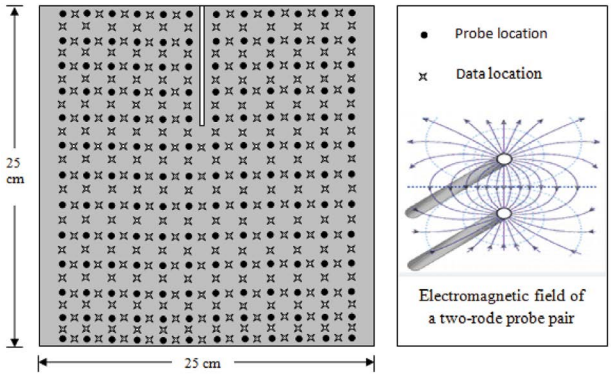

Figure 10. A schematic diagram of the location of data collection.

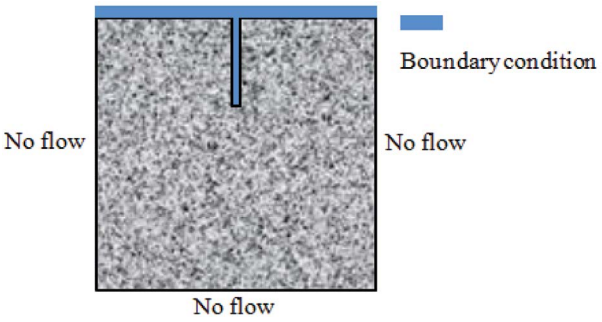

Figure 11. Model boundary conditions.

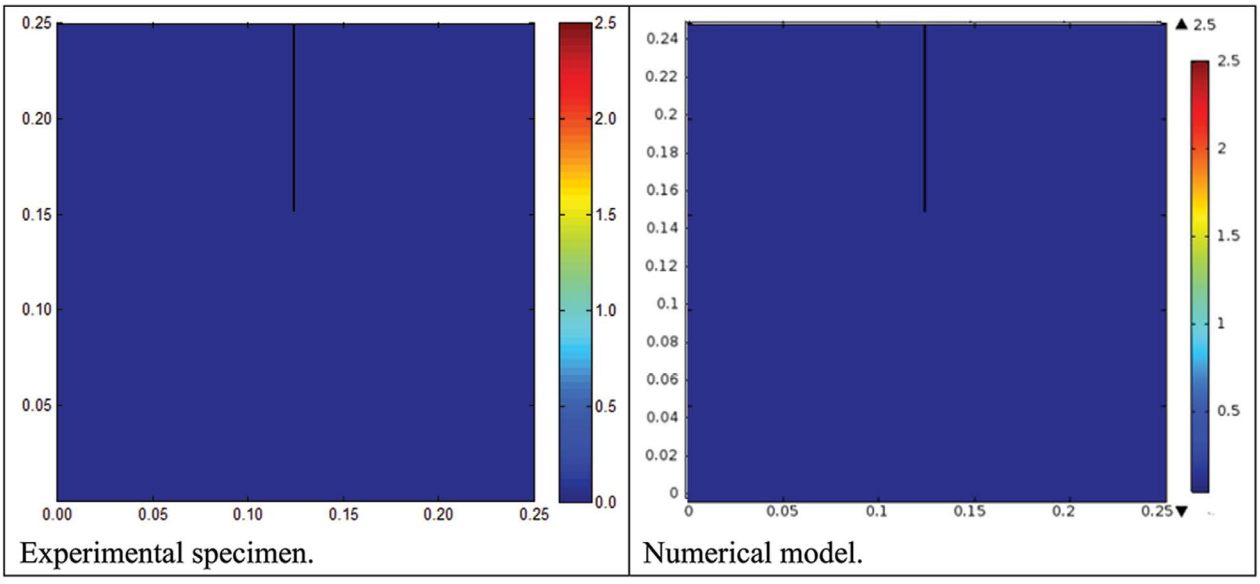

Figure 12. Experimental and numerical results at 0 hour.

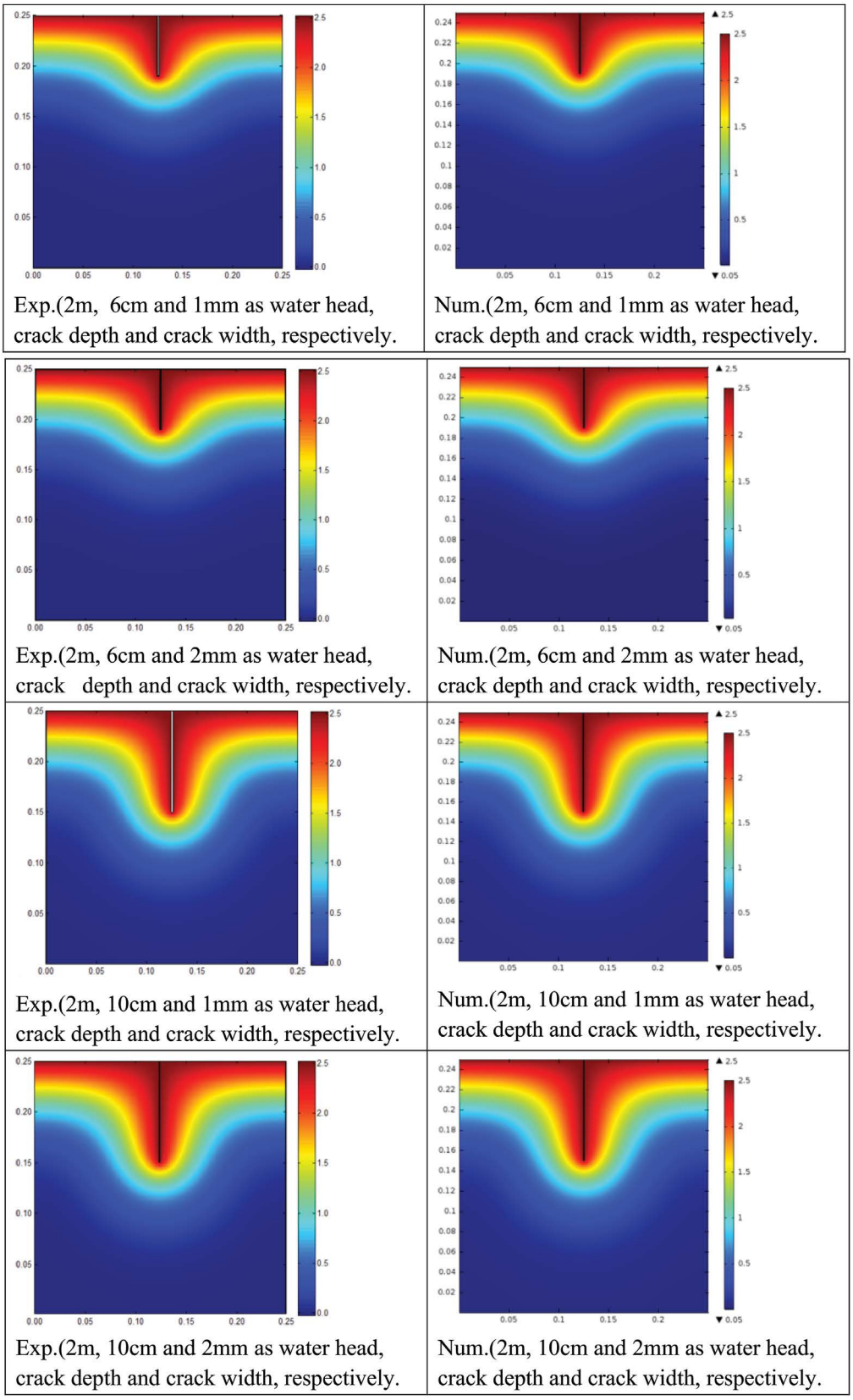

Figure 13. Experimental and numerical results after 312 hours of the exposure conditions

system, the top line and crack line were exposed to solute chloride in water as boundary conditions. The other boundaries had a no flow condition imposed to represent an impermeable coating on the real specimens.

The initial chloride concentration inside the concrete was assigned to be 0.05 for all the analyses, due to the concentration values were measured at time 0 hr. of the EC test. The data matrices reported in the chloride concentrations of calibration samples which tested by the ECT were linearly interpolated automatically to the node resolution of the model, so that chloride concentration values outside of the data matrix were extrapolated to be a constant value (2.5%) as the maximum boundary of the concentration data matrix. The time dependent solver was used to solve the model with 0 and 312 hours of exposing to request boundary conditions.

5. Comparison of Results

After tested and gotten the results of the numerical models and experimental specimens. The comparing between them was done and as shown in Figure (12 a-b). The crack forms are shown as a straight line at the middle position of images.

After analyzing the above experimental and numerical results are shown in Figure 13, it can be concluded that the chloride penetration depth is increasing with an increasing crack width and crack depth, where the most influential factors of the crack width and crack depth, on the concentration of penetration chloride, was share of the crack width. Crack depths with widths, for the same exposure of water head, were not having a significant effect on chloride penetration depth. This probably due to the recently used of concrete mixture of specimens.

6. Conclusions

In this paper, the influence of crack sizes (depth and width) on the chloride penetration in Hydraulic Concrete Structures, which exposed to seawater head, is experimentally and numerically studied. Following are the final conclusions that can be inferred:

- The chloride penetration depth increased with increased crack width and crack depth, respectively.
- Comparisons between the experimental and numerical results concluded that the numerical ones, which obtained using Finite Element analysis (COMSOL Multiphysics Software), agreed well with the experimental ones which gained from experiment tests for the cracked specimens.
- The developed ECT is the more suitable method for determining the degree of saturation and penetration of chloride ions into laboratory concrete specimens for the following reasons: 1. Typical and very accurate results comparing with numerical results, 2. The experimental data could be used to determine the necessary parameters required in specimens when predicting the transport of chlorides in concrete specimens and 3. The experimental has a low cost, easy set-up and the experiment can be performed in a very short time compared to other experiments.

7. References

1. Frederiksen J, Sorensen H, Andersen A, Hetek Klinghoffer O. The effect of the w/c ratio on chloride transport into concrete. Immersion, migration and resistivity tests. Technical Report. 1997. p. 1-94.
2. Jaffer S, Hansson C. Chloride-induced corrosion products of steel in cracked-concrete subjected to different loading conditions. Cement and Concrete Research. 2009; 39(2):116-25. https://doi.org/10.1016/j.cemconres.2008.11.001
3. Gowripalan N, Sirivivatnanon V, Lim C. Chloride diffusivity of concrete cracked in flexure. Cement and Concrete Research. 2000; 30(5):725-73. https://doi.org/10.1016/S0008-8846(00)00216-7
4. Malhotra V, Carino N. Handbook on Nondestructive Testing of Concrete. 2nd ed. CRC Press; 2003. p. 1-384. https://doi.org/10.1201/9781420040050
5. Whiting D, Nagi M. Electrical resistivity of concrete-a literature review. R&D Serial. 2003. p. 1-57.
6. Monteiro P. Concrete: Microstructure, properties, and materials. 3rd ed. McGraw-Hill Publishing; 2006. p. 1-659.
7. Whittington H, McCarter J, Forde M. The conduction of electricity through concrete. Magazine of Concrete Research. 1981; 33(114):48-60. https://doi.org/10.1680/macr.1981.33.114.48
8. Newlands M, Jones M, Kandasami S, Harrison T. Sensitivity of electrode contact solutions and contact pressure in assessing electrical resistivity of concrete. Materials and Structures. 2008; 41:1-621. https://doi.org/10.1617/s11527-007-9257-6
9. Spragg R, Castro J, Nantung T, Paredes M, Weiss J. Variability analysis of the bulk resistivity measured using concrete cylinders. Advances in Civil Engineering Materials. 2012;1(1):1-17.

https://doi.org/10.1520/ACEM-2012-0004 https://doi.org/10.1520/ACEM104596
10. Wenner F. A method for measuring earth resistivity. Journal of the Washington Academy of Sciences. 1915; 5:561-3.
11. Polder R, Andrade C, Elsener B, Vennesland O, Gulikers J, Weidert R. Test methods for on site measurement of resistivity of concrete. Materials and Structures. 2000; 33(10):603-11. https://doi.org/10.1007/BF02480599
12. Andrade C, Polder R, Basheer M. Non-destructive methods to measure ion migration. RILEM Publications SARL; 2007. p. 91-112.
13. Liu Y, Suarez A, Presuel-Moreno F. Characterization of new and old concrete structures using surface resistivity measurements. Florida Department of Transportation Research Center, Final Report, Florida. 2010.
14. Rupnow T, Icenogle P. Surface resistivity measurements evaluated as alternative to rapid chloride permeability test for quality assurance and acceptance. Transportation Research Record: Journal of the Transportation Research Board. 2012; 2290:30-7. https://doi.org/10.3141/2290-04
15. Du Plooy R, Lopes S, Villain G, Derobert X. Developed of a multi-ring resistivity cell and multi-electrode resistivity probe for investigation of cover. NDT & E International. 2013; 54:27-36. https://doi.org/10.1016/j.ndteint.2012.11.007
16. Adiyastuti S. Influence of cracks on chloride induced corrosion in reinforced concrete flexural members. University of New South Wales; 2005.
17. Luping T, Nilsson L, Basheer P. Resistance of concrete to chloride ingress. London: Taylor and Francis; 2012.
18. Freeze R, Cherry J. Groundwater. Englewood Cliffs, NJ: Printice-Hall Inc.; 1979. p. 1-604.
19. Niwa A, Clough R. Shaking table research on concrete dam models. Earthquake Engineering Research Center: University of California; 1980. p. 1-126.
20. Otieno M, Alexander M, Beushausen H. Corrosion in cracked and uncracked concrete–influence of crack width, concrete quality and crack reopening. Magazine of Concrete Research. 2010; 62(6):393-404. https://doi.org/10.1680/macr.2010.62.6.393
21. Blagojevic A. The influence of cracks on the durability and service life of reinforced concrete structures in relation to chloride-induced corrosion: A look from a different perspective. TU Delft, Delft University of Technology; 2016.
22. Safehian M, Ramezanianpour A. Assessment of service life models for determination of chloride penetration into silica fume concrete in the severe marine environmental condition. Construction and Building Materials. 2013; 48:287-94. https://doi.org/10.1016/j.conbuildmat.2013.07.006
23. Monfore G. The electrical resistivity of concrete. Journal of the Portland Cement Association. Skokie, IL: Research and Developed Laboratories. 1968; 10:35-48.
24. Hansson I, Hansson C. Electrical resistivity measurements of Portland cement based materials. Cement and Concrete Research. 1983; 13(5):675-83. https://doi.org/10.1016/0008-8846(83)90057-1
25. Saleem M, Shameem M, Hussain S, Maslehuddin M. Effect of moisture, chloride and sulphate contamination on the electrical resistivity of Portland cement concrete. Construction and Building Materials. 1996; 10(3):209-14. https://doi.org/10.1016/0950-0618(95)00078-X
26. Weiss J, Snyder K, Bullard J, Bentz D. Using a saturation function to interpret the electrical properties of partially saturated concrete. Journal of Materials in Civil Engineering. 2012; 25(8):1097-106. https://doi.org/10.1061/(ASCE)MT.1943-5533.0000549
27. Atkinson A, Nickerson A. The diffusion of ions through water-saturated cement. Journal of Materials Science. 1984; 19(9):3068-78. https://doi.org/10.1007/BF01026986
28. Garboczi E. Permeability, diffusivity, and microstructural parameters: A critical review. Cement and Concrete Research. 1990; 20(4):591-601. https://doi.org/10.1016/0008-8846(90)90101-3
29. Korhonen C, Janoo V, Berini C. Time-domain reflectometry of water content in Portland cement concrete. Hanover: Cold Regions Research and Engineering Lab; 1997. p. 1-23